

We are IntechOpen, the world's leading publisher of Open Access books Built by scientists, for scientists

4,800

Open access books available

122,000

International authors and editors

135M

Downloads

Our authors are among the

154

Countries delivered to

TOP 1%

most cited scientists

12.2%

Contributors from top 500 universities

**WEB OF SCIENCE™**Selection of our books indexed in the Book Citation Index
in Web of Science™ Core Collection (BKCI)

Interested in publishing with us?
Contact book.department@intechopen.com

Numbers displayed above are based on latest data collected.

For more information visit www.intechopen.com

Rapid Calculation of Residual Notch Stress Intensity Factors (R-NSIFs) by Means of the Peak Stress Method

Marco Colussi, Paolo Ferro, Filippo Berto and
Giovanni Meneghetti

Additional information is available at the end of the chapter

<http://dx.doi.org/10.5772/intechopen.73514>

Abstract

The intensity of the residual singular stress distribution can be quantified by the residual notch stress intensity factor (R-NSIF), which might be a useful stress parameter to include in local approaches for fatigue strength assessments of welded joints. In order to calculate the residual stress fields by means of welding process simulations, the mesh adopted in numerical models has necessarily to be very fine. Unfortunately, the nonlinear and transient behavior of the welding simulation makes numerical analyses extremely demanding in terms of computational time, particularly, if large welded structures and/or multipass welds have to be simulated. In this scenario, the use of methods aimed at reducing the computational effort to estimate local stresses and strains in welded structures can be effective. Among these, the peak stress method has been proposed to estimate the notch stress intensity factors (NSIFs) at sharp V-notches, using coarse finite element patterns. In this work, the peak stress method (PSM) has been used to calculate the R-NSIF of a full penetration welded T-joint. It has been shown that the PSM can successfully be used to estimate R-NSIFs values, provided that the stress redistribution induced by plasticity in the zone very close to the notch tip is negligible.

Keywords: residual notch stress intensity factor, residual stress, peak stress method, finite element analysis, coarse mesh

1. Introduction

Residual stresses are induced on fusion-welded joints as a consequence of thermal gradients and nonuniform plastic deformations during the cooling phase. According to clamping conditions, process parameters and kind of alloys to be welded, they can be negative or positive. Positive, or tensile residual stresses, are known to be detrimental for the high cycle fatigue strength joints [1, 2], whereas their effect on low cycle fatigue resistance is found negligible or null, as well. This is because the higher the stress amplitude, the higher the extension of plastic deformation in the fatigue crack initiation sites (weld toe or weld root) that cancels the preexisting residual stress state. On the other hand, negative residual stresses induced by fusion welding have been found to increase the fatigue strength of joints [3] and thus are considered beneficial for the joint itself. Residual stress effect on fatigue strength of welded components is implicitly taken into account by design fatigue curves obtained from experimental data generated by testing welded joints prepared with different process parameters. Despite this current methodology, new design approaches that take into account residual stress explicitly were published in recent literature [4–8]. Hensel et al. proposed a method that replaces the nominal stress ratio with the effective stress ratio to describe the combined effect of mean and residual stresses. Ferro [4], on the other hand, suggested the use of the strain energy density (SED) approach [9] to quantify the residual stress effect on fatigue strength of welded joints through the assessment of residual notch stress intensity factors (R-NSIFs). The analysis of residual stress distribution has been a challenging task since many years. The *a posteriori* assessment of residual stress can be performed by experimental techniques, though they are time-consuming and expensive and provide data at single points (in most cases at the surface) of the joint. *A priori* residual stress determination can be obtained by numerical models, yet they need to be validated. Welding simulations are very complex because fluid dynamics, metallurgical, thermal and mechanical phenomena interact with each other [10]. When residual stress and strain are the major goals of the simulation, fluid dynamics of welding pool is almost always not taken into account. In these cases, the fusion zone is modeled by power density distribution functions whose shape and dimensions depend on welding technology (laser welding, arc welding and so on) and process parameters, respectively. Furthermore, the analysis is transient and nonlinear [11]. Numerical models require high mesh densities in order to capture the severe thermal gradient induced by the welding source. Moreover, in real components, multipass welding is often adopted. Promising approaches are already present in literature, but not yet extensively validated. In the ‘macroweld deposit approach’, the heat is applied in a welding instantaneously, without using a power source. The macrosteps number is chosen a priori based on the experience and real welding speed. The higher the welding speed, the longer is the single macrostep. The heat transferred into the structure is the same as in the real process, but it occurs in another time frame. In contrast to the macroweld deposit methodology, with the local-global method, the welding simulation is carried out on a refined local model (LM), whose geometry is extracted from the global structure (GS). The nodal displacements coming from LM solution are applied to the GS and a linear elastic computation is finally performed to assess the global distortion. The mesh can be locally refined and the refined zone follows the welding source by saving

computational time. Models with coupled 3D and shell elements are also used to simplify the analysis. The bead is modeled with 3D elements, while the plates are modeled with shell elements. Finally, a 2D model can also be used to simplify the simulation. In this case, the welding source is thought to pass across the modeled cross section and melting the alloy. Stress and strain are computed under generalized plain strain condition. In previous works, it has been demonstrated that if the weld toe is modeled as a sharp, zero radius, V-shaped notch, residual stress field near that zone is singular [12–14] and its sign depends on both clamping conditions and metallurgical characteristics of the alloy to be welded [13, 14]. This outcome of numerical simulations allows to treat the asymptotic residual stress field like the load-induced singular stress field by means of the R-NSIF (residual-notch stress intensity factor), i.e., a stress field parameter able to quantify the intensity of the residual stresses near the weld toe. Because, direct R-NSIF calculation from asymptotic local stress fields requires very fine meshes, new strategies are needed to speed up numerical analysis. In this context, the peak stress method (PSM) has been proved to be suitable for the notch stress intensity factors (NSIFs) calculation by means of coarse meshes [15]. Therefore, in the present work, the use of the PSM is validated also for the R-NSIFs assessment.

2. Analytical background of the peak stress method

The peak stress method (PSM) is an engineering, FE-based method to estimate the notch stress intensity factors (NSIFs) at the weld toe and at the weld root of welded joints. The basic idea is to use very coarse meshes, if compared with those required to evaluate directly the asymptotic stress distributions required to apply the NSIFs definitions. The second peculiarity of the method is that the sole linear elastic peak stress evaluated at the sharp V-notch tip is necessary and sufficient to estimate the NSIF: therefore, the singular stress fields do not need to be postprocessed according to the NSIFs definitions (Eqs. (1) and (2)). Both these features of the method make it useful in practical applications.

In plane problems, the local linear elastic stress fields close to the tip of sharp V-notches, like those shown in the welded joint of **Figure 1**, can be expressed as functions of the relevant NSIFs, which quantify the magnitude of the asymptotic singular stress distributions. The asymptotic, singular stress distributions ahead of sharp V-notches under mode I (opening) and mode II (sliding) loadings have been determined by Williams [16]. The mode I and mode II NSIFs can be defined according to Gross and Mendelson [17] by means of Eqs. (1) and (2), respectively.

$$K_1 = \sqrt{2\pi} \cdot \lim_{r \rightarrow 0} [(\sigma_{\theta\theta})_{\theta=0} \cdot r^{1-\lambda_1}] \quad (1)$$

$$K_2 = \sqrt{2\pi} \cdot \lim_{r \rightarrow 0} [(\tau_{r\theta})_{\theta=0} \cdot r^{1-\lambda_2}] \quad (2)$$

The stress singularity exponents λ_1 and λ_2 depend on the notch opening angle 2α [16] and are reported in **Table 1**. The stress components $\sigma_{\theta\theta}$ and $\tau_{r\theta}$ are calculated along the direction $\theta = 0$, i.e., the notch bisector (see **Figure 1**).

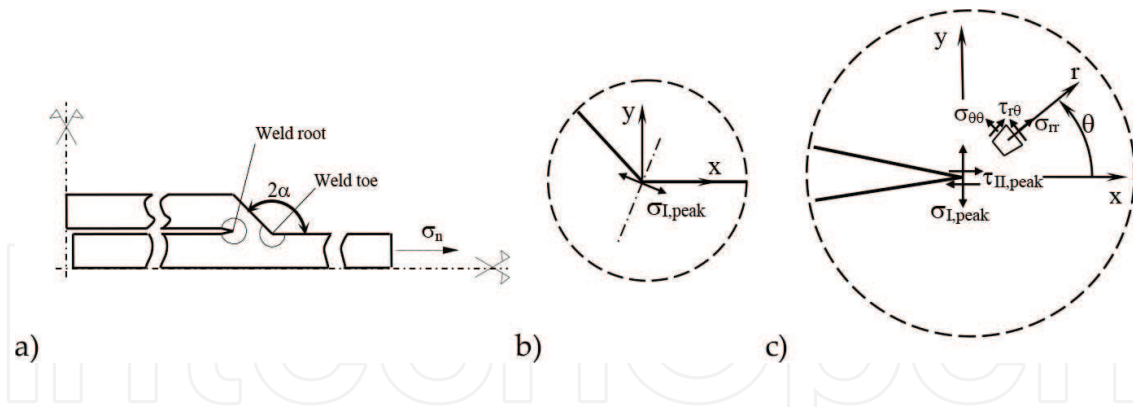


Figure 1. Sharp V-shaped notches in a welded joint (a) at the toe (2α typically equal to 135°) (b) and at the root ($2\alpha = 0^\circ$) (c) sides. Definition of peak stresses $\sigma_{I,peak}$ and $\tau_{II,peak}$ evaluated at the weld toe and the weld root by means of a linear elastic finite element analysis.

2α (deg)	λ_1	λ_2
0	0.500	0.500
90	0.544	0.909
135	0.674	

Table 1. Values of the stress singularity exponents λ_1 and λ_2 .

Notch stress intensity factors (NSIFs) proved to correlate the static strength of components made of brittle or quasi-brittle materials and weakened by sharp V-notches [18–23], as well as the medium and high-cycle fatigue strength of notched components made of structural materials [24, 25]. Concerning welded joints, NSIFs have been used to analyze the fatigue strength both under uniaxial [26–30] and multiaxial cyclic loadings [31]. However, to apply the NSIF approach by means of finite element (FE) analyses in engineering problems, a major drawback arises, because of the very refined FE meshes needed to evaluate the NSIFs on the basis of the definitions reported in Eqs. (1) and (2). In the case of three-dimensional components, the numerical analyses are even more time-consuming.

Recently, a simplified and rapid technique, the so-called peak stress method (PSM), has been proposed in order to speed up the numerical evaluation of the NSIFs by adopting FE models with coarse meshes. Inspired by previous contributions by Nisitani and Teranishi [32, 33] to rapidly estimate the mode I SIF of cracks, the PSM has been theoretically justified and extended to estimate also the mode I NSIF of pointed V-notches [34, 35]; subsequently, it has been formulated for the mode II SIF of cracks [36] and the mode III NSIF of pointed V-notches [37].

Essentially, the PSM allows to rapidly estimate the NSIFs K_1 and K_2 (Eqs. (1) and (2)) from the singular, linear elastic, opening (mode I) and sliding (mode II) FE peak stresses $\sigma_{I,peak}$ and $\tau_{II,peak}$ respectively, which are calculated at the node located at the V-notch tip (see **Figure 1**) by means of an FE analysis in which the following parameters are calibrated:

- the adopted FE code;
- the element type and formulation;

- the FE mesh pattern;
- the criteria for stress extrapolation at FE nodes.

In more detail, the expressions of the PSM are the following [34, 36]:

$$K_1 \cong K_{FE}^* \cdot \sigma_{I,peak} \cdot d^{1-\lambda_1} \quad (3)$$

$$K_2 \cong K_{FE}^* \cdot \tau_{II,peak} \cdot d^{0.5} \quad (4)$$

In previous expressions, d is the so-called global element size parameter to input in the FE software, i.e., the mean size of the finite elements adopted by the free mesh generation algorithm available in the numerical code, while K_{FE}^* and K_{FE}^{**} take into account all calibration parameters mentioned previously.

With reference to plane models, the PSM has been calibrated [34, 36] under the following conditions:

- Adopted FE code: Ansys
- Element types (element library of Ansys code):
 - Two-dimensional, 4-node quadrilateral finite elements with linear shape functions (PLANE 42 or alternatively PLANE 182 with K-option 1 set to 3, i.e., ‘*simple enhanced strain*’ formulation activated).
 - Three-dimensional, eight-node brick elements (SOLID 45 or equivalently SOLID 185 with K-option 2 set to 3, i.e., ‘*simple enhanced strain*’ option activated).
 - Two-dimensional, harmonic, 4-node linear quadrilateral elements, to analyze axis-symmetric components subjected to external loads that can be expressed according to a Fourier series expansion (PLANE 25).
- There is a standard mesh pattern close to the V-notch or crack tip that is reported in **Figure 2** [34, 36], where it is seen that four elements share the node located at the notch tip if the notch opening angle 2α is equal to or lower than 90° ; conversely, if the notch opening angle is $2\alpha > 90^\circ$, then two elements share the node at notch tip. **Figure 2** shows examples of such mesh patterns in case of symmetric FE models. It should be noted that the mesh patterns according to the PSM are automatically generated by the *free-mesh generation algorithm* of Ansys code, after having input the average FE size d by means of the command ‘global element size’ available in the software. There are not additional parameters or special settings to input in order to generate the mesh.
- Eq. (3) can be applied to sharp V-notches with an opening angle 2α between 0° and 135° ; while calibration for mode II loading, Eq. (4), is restricted to the crack case ($2\alpha = 0$, $(1 - \lambda_2) = 0.5$).

Under these conditions, the following values have been calibrated: $K_{FE}^* \cong 1.38$ and $K_{FE}^{**} \cong 3.38$. To apply expressions (3) and (4) with $K_{FE}^* = 1.38$ and $K_{FE}^{**} = 3.38$, the average element size d can be chosen arbitrarily, but within a range of applicability defined in the relevant literature

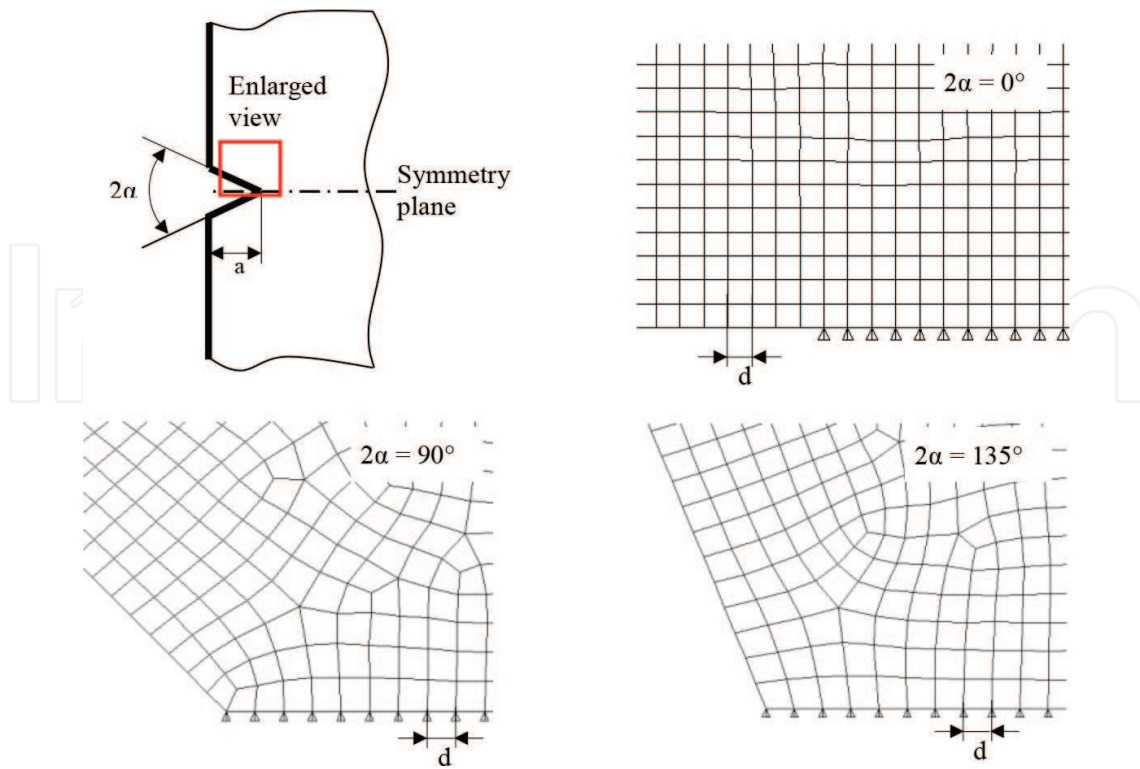


Figure 2. Mesh patterns according to the PSM [34, 36]. Symmetry boundary conditions are applied to the FE model.

[34, 36]: for mode I loading (Eq. (3)), the mesh density ratio a/d that can be adopted in FE analyses must exceed 3 to obtain $K_{FE}^* = 1.38 \pm 3\%$; in case of mode II loading (Eq. (4)), more refined meshes are needed, the mesh density ratio a/d having to be greater than 14 to obtain $K_{FE}^{**} = 3.38 \pm 3\%$. In previous expressions, a is the characteristic size of the analyzed sharp V-notch, i.e., the notch depth in **Figure 2**. In case of welded T-joints analyzed at the weld toe side, a is the main plate thickness ($a = 6$ mm in next **Figure 3**).

Any structural strength assessment criterion, which is based on NSIF parameters, could be reformulated by using the PSM by means of Eqs. (3) and (4). In the recent literature, the PSM has been coupled to the averaged strain energy density (SED) criterion to assess the fatigue strength of welded joints subjected to axial [15, 36, 38, 39], torsion [37, 40] and multiaxial [41, 42] loading conditions.

3. R-NSIFs evaluation by using the peak stress method

The PSM has been recently calibrated in Sysweld[®] finite element environment, to rapidly evaluate the linear elastic notch stress intensity factor (NSIF) under mode I loading [43]. According to such calibration, the mode I NSIF is proportional to a constant K_{FE}^* , which is equal to 1.64 in case of V-notches with opening angle ranging from 90° to 135° and equal to 1.90 in case of cracks (0° opening angle). Provided that the mesh density ratio is equal to or greater than 4, all FE results fall within a scatter band of $\pm 5\%$, regardless of the V-notch depth.

The aim of this section is to show the procedure of R-NSIFs evaluation through the PSM with a practical application. With this purpose, a full penetration welded T-joint has been analyzed using the finite element code Sysweld[®]. Generalized plane strain condition has been assumed, this choice being appropriate to describe the out-of-plane stress values in 2D cross section model of welding process [44]. The welded joint geometry and the assumed dimensions are shown in **Figure 3**.

According to the PSM hypothesis, the weld toe has been modeled as a sharp, zero radius, V-shaped notch. The notch opening angle 2α has been chosen equal to 135° . It has been assumed carbon steel with chemical composition according to the Standard ASTM SA 516 (Grade 65 resp. 70) and the corresponding thermomechanical properties have been taken from Sysweld[®] database. Thermometallurgical and mechanical properties as a function of phase and temperature have been taken into account (Sysweld Toolbox 2011). In the metallurgical analysis, the following phases have been included: martensite, bainite, and ferrite-pearlite. The metallurgical transformations mainly depend on thermal history, according to the continuous cooling transformation (CCT) diagrams, which plot the start and the end transformation temperatures as a function of cooling rate or cooling time. In the present work, the diffusion-controlled phase transformations and the displacive martensitic transformation have been modeled according to Leblond and Devaux [45] and to Koistinen and Marburger [46] kinetic law, respectively. Radiative and convective heat losses have been applied at the boundary (external surfaces) of the plates to be joined—the former by using the Stefan-Boltzman law and the latter by using a convective heat transfer coefficient equal to $25 \text{ W/m}^2 \text{ K}$. The thermal gradient in the out-of-plane direction cannot be taken into account in a 2D cross section model because of its intrinsic formulation. However, it is supposed that the higher the welding speed, the lower the out-of-plane thermal gradient. The thermal history at nodes of the numerical model is the only load applied in welding simulation. Such thermal load is simulated by means of a power density distribution function whose shape depends on welding technology. In this work, the heat source has been modeled using a double ellipsoid power density distribution function [47] described by Eq. (5), which has been widely used in literature for arc welding simulation [10].

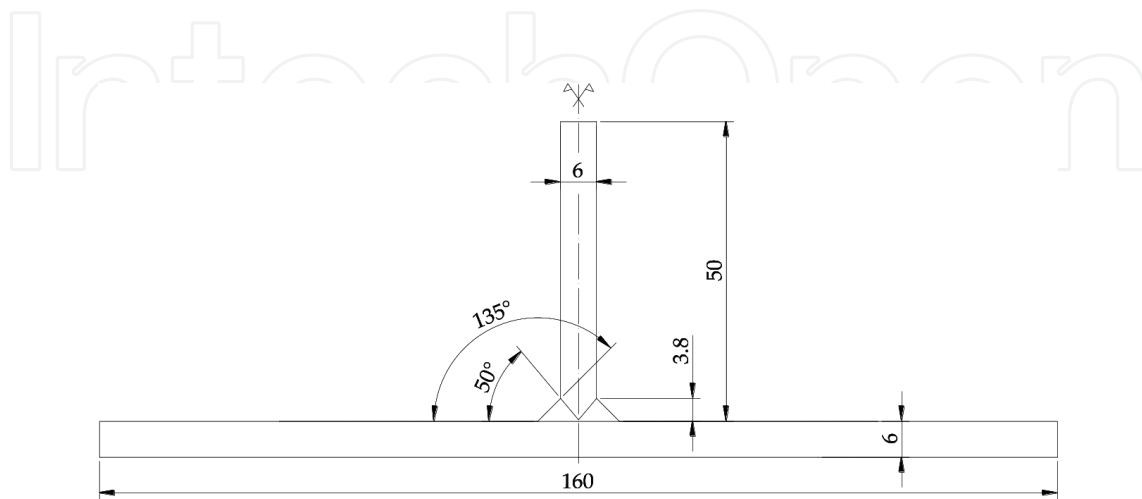


Figure 3. Schematic representation of the T-joint. Dimensions are in mm.

$$q(x, y, t) = \frac{6\sqrt{3} f_{1,2} Q}{\pi\sqrt{\pi} a_0 b_0 c_{1,2}} e^{-\frac{3x^2}{a_0^2}} e^{-\frac{3y^2}{b_0^2}} e^{-\frac{3[v(\tau-t)]^2}{c_{1,2}^2}} \tag{5}$$

The double ellipsoid heat source and the meaning of the symbols used in Eq. (5) are shown in **Figure 4**, whereas the adopted numerical values are summarized in **Table 2**. The power density provided by Eq. (5) has the unit W/m³.

By taking advantage on the symmetry, one-half of the joint has been modeled. In **Table 3**, the very refined mesh pattern used in the calculation of R-NSIF from the local stress field and the

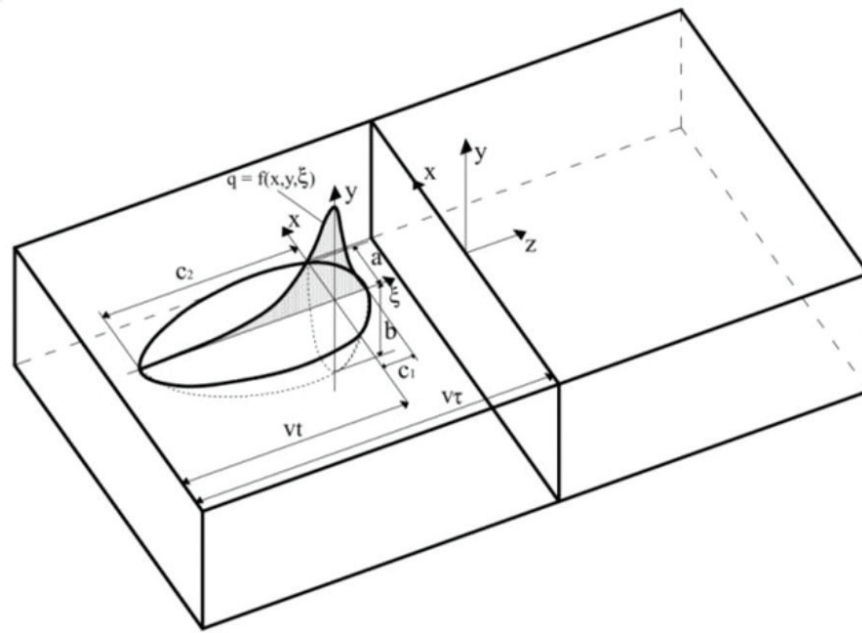


Figure 4. Schematic of Goldak’s heat source with symbols taken from the original paper [45].

Q^*	Power input [W]	11,500
η	Efficiency	0.64
Q	Absorbed power [W]	$\eta \cdot Q^*$
a_0	Molten pool dimensions [mm]	3.5
b_0		11
c_1		2.3
c_2		7.9
f_1	Fractions of heat deposit in the front and rear quadrants, with $f_1 + f_2 = 2$	0.6
f_2	(subscript 1 for $\xi > 0$; subscript 2 for $\xi < 0$)	1.4
v	Welding speed [mm/s]	11
τ	Total time before the welding torch is over the transverse cross section [s]	3

Table 2. Goldak’s source parameters adopted in the present analysis.

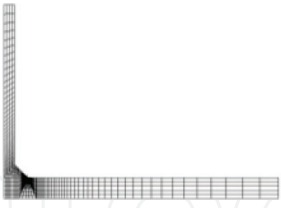
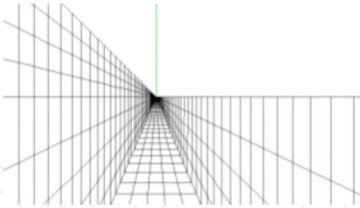

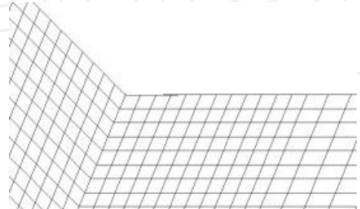
Method	Global FEM model	Detail of mesh refinement near the weld toe	R-NSIF value [MPa mm ^{0.326}]	N° of FE in model	Δ %
Local stress filed calculation			52.4	2500	—
PSM			52.9	1350	0.9

Table 3. Finite element meshes used to directly compute the R-NSIF from local stress and to estimate it by using the PSM.

typical free-generated mesh pattern according to the PSM evaluation are compared. The FE model used to compute R-NSIFs from local stress fields had a minimum element size at the notch tip equal to about 5×10^{-5} mm, according to the literature [27].

The FE models used to estimate the R-NSIFs by means of the PSM were generated by using a mesh pattern as similar as possible to the standard PSM shown in **Figure 2**, according to the PSM calibration rules for Sysweld[®] finite element code listed in the previous section. The mesh generation algorithm provided by visual mesh has been adopted. Four-node 2004 quadrilateral elements from Sysweld library have been used and the numerical integration scheme was set to 2×2 Gauss points. The average finite element size d imposed to the mesh generation algorithm is 0.29 mm, which translates into a mesh density ratio a/d equal to 10. Such FE size was necessary to obtain a temperature field in agreement with that obtained with the very refined mesh pattern. More precisely, to establish the appropriate d value, a difference in nodal temperatures of few percentage points was allowed between the very refined and the PSM coarse meshes. Uncoupled thermomechanical analyses were carried out, where the molten effect was simulated by using a specific function implemented in Sysweld code that cancels the history of an element if its temperature exceeds the melting temperature. Welded plates have been supposed free of restraints, except for the symmetry boundary condition.

4. Results and discussion

The asymptotic nature of the residual stress distribution near a sharp V-notch has been numerically investigated by using Sysweld[®]. **Figure 5** shows the temperature distribution when the melted zone has reached its maximum extension. It has been found that the stress

distribution near the weld toe is linear in a log-log plot (**Figure 6**) and its slope is equal to 0.326, which corresponds to the analytical solution for open V-notches with zero radius. The intensity of such residual stress field can therefore be given in terms of R-NSIFs.

Concerning the PSM, a peak stress value equal to 48.3 MPa was calculated at the node located at the weld toe. A mesh pattern having element size equal to 0.29 mm was adopted near the weld toe, which corresponds to a mesh density ratio $a/d = 10 \geq 4$, according to the PSM calibration in Sysweld[®] [43]. Results are summarized in **Table 3**, where it is possible to notice a good agreement between the K_I value obtained from the local stress field computed with a very fine mesh and the one estimated by means of the coarse PSM mesh. In the latter case, the PSM calibration constant for $K_{FE}^* = 1.64$, valid for Sysweld[®], has been used.

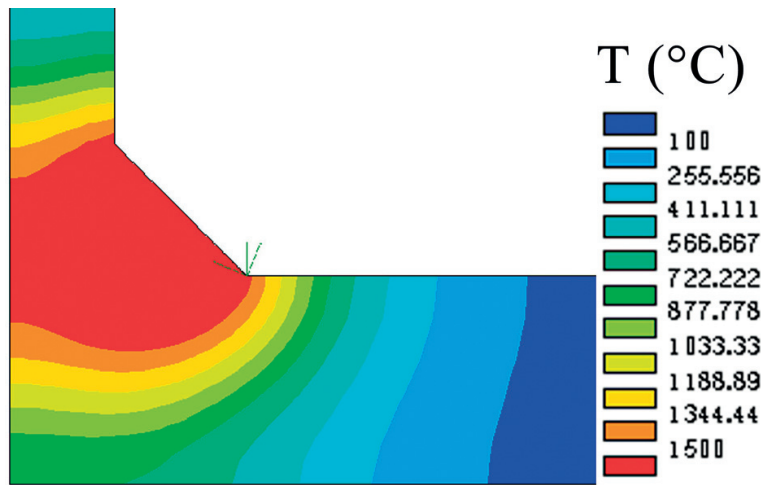


Figure 5. Temperature distribution at the instant of maximum width of the fusion zone (in red).

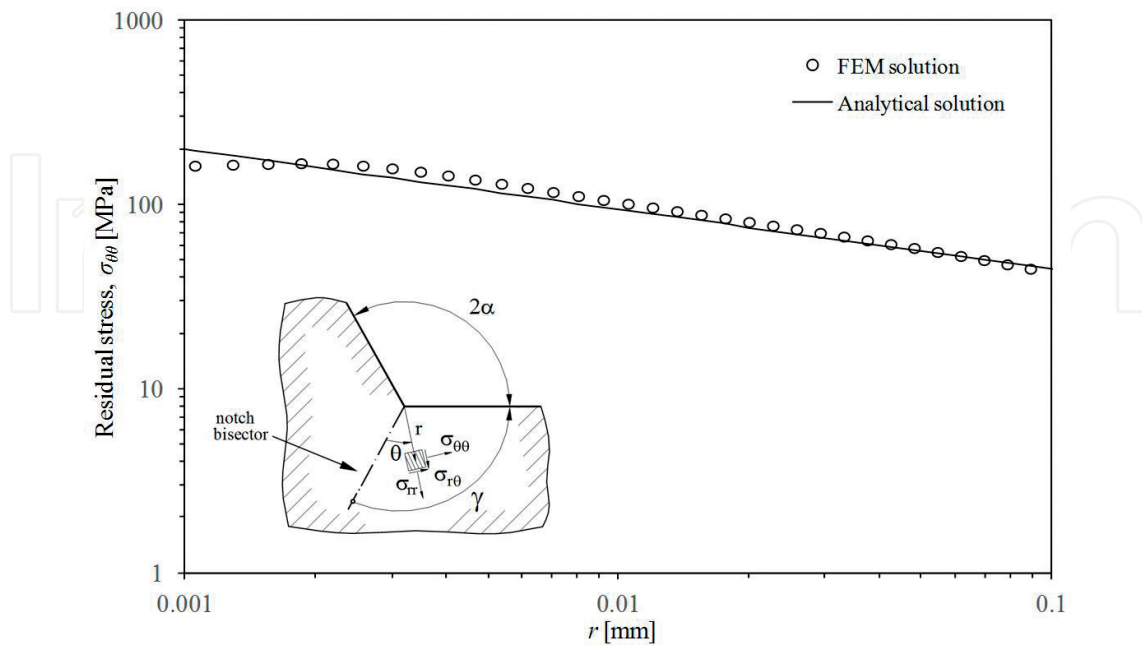


Figure 6. Asymptotic $\sigma_{\theta\theta}$ component of the residual stress field near the notch tip along the notch bisector, i.e., $\theta = 0^\circ$.

This investigation confirms that the PSM can be used for a rapid, engineering R-NSIF evaluation. To illustrate the advantage of the PSM, the solution time associated to the very refined meshes was about 1 min for thermal analyses and 4 min for mechanical analyses, whereas the PSM required few seconds for thermal analyses and a minute for mechanical analyses. Moreover, the following main advantages can be exploited if the R-NSIFs are estimated by means of the PSM rather than directly computed from local stress fields: (a) only one nodal stress value calculated at the point of singularity is sufficient to compute the R-NSIF, the whole stress distribution along the notch bisector being no longer required; (b) four orders of magnitude coarser meshes could be employed by using the PSM, as compared to the very refined meshes required to evaluate the local stress field directly. In the authors' opinion, both reasons make the PSM of easy and fast applicability in industrial and research applications. Finally, the PSM appears also suitable, with further developments and investigation, for the R-NSIF value calculation by using three-dimensional FE models of welding process.

5. Conclusions

In the present contribution, a practical application of the PSM in the residual notch stress intensity factor (R-NSIF) estimation on a full penetration welded T-joint has been given. It has been found that, provided that the stress redistribution induced by plasticity in the zone very close to the notch tip is negligible, the PSM allows the rapid, coarse mesh-based, estimation of the R-NSIF. This result is promising because, in principle, R-NSIFs may be useful parameters to include the residual stress effect in fatigue strength assessments of welded joints.

Author details

Marco Colussi¹, Paolo Ferro¹, Filippo Berto² and Giovanni Meneghetti^{3*}

*Address all correspondence to: giovanni.meneghetti@unipd.it

1 Department of Engineering and Management, University of Padova, Vicenza, Italy

2 Department of Industrial and Mechanical Engineering, Norwegian University of Science and Technology, Trondheim, Norway

3 Department of Industrial Engineering, University of Padova, Padova, Italy

References

- [1] Livieri P, Lazzarin P. Fatigue strength of steel and aluminium welded joints based on generalised stress intensity factors and local strain energy values. *International Journal of Fracture*. 2005;133:247-278

- [2] Gurney TR. *The Fatigue Strength of Transverse Fillet Welded Joints*. Cambridge: Abington Publishing; 1991
- [3] Bertini L, Fontanari V, Straffellini G. Influence of post weld treatments on fatigue behaviour of Al-alloy welded joints. *International Journal of Fatigue*. 1998;**20**:749-755
- [4] Ferro P. The local strain energy density approach applied to pre-stressed components subjected to cyclic load. *Fatigue and Fracture of Engineering Materials and Structures*. 2014;**37**:1268-1280
- [5] Ferro P, Berto F, James MN, Borsato T. Review of recent advances in local approaches applied to pre-stressed components under fatigue loading. In: Iacoviello F, Susmel L, Firrao D, Ferro G, editors. *21st European Conference on Fracture*; 20–24 June 2016; Catania. Elsevier; 2016
- [6] Ferro P, Berto F, James NM. Asymptotic residual stresses in butt-welded joints under fatigue loading. *Theoretical and Applied Fracture Mechanics*. 2016;**83**:114-124
- [7] Ferro P, Berto F. Quantification of the influence of residual stresses on fatigue strength of Al-alloy welded joints by means of the local strain density approach. *Strength of Materials*. 2016;**48**:426-436
- [8] Hansel J, Nitschke-Pagel T, Dilger K. Engineering model for the quantitative consideration of residual stresses in fatigue design of welded components. *Welding in the World*. 2017;**61**:997-1002
- [9] Lazzarin P, Zambardi R. A finite-volume-energy based approach to predict the static and fatigue behavior of components with sharp V-shaped notches. *International Journal of Fatigue*. 2001;**112**:275-298
- [10] Ferro P, Bonollo F, Tiziani A. Methodologies and experimental validations of welding process numerical simulation. *International Journal of Computational Materials Science and Surface Engineering*. 2010;**3**:114-132
- [11] Ferro P. Molten pool in welding processes: Phenomenological vs fluid-dynamic numerical simulation approach. In: Arnberg L, Bonollo F, Montanari R, editors. *Liquid Metals and Alloys: From Structure to Industrial Applications*. Switzerland: Trans Tech Publications Ltd; 2017
- [12] Ferro P, Berto F, Lazzarin P. Generalized stress intensity factors due to steady and transient thermal loads with applications to welded joints. *Fatigue and Fracture of Engineering Materials and Structures*. 2006;**29**:440-453
- [13] Ferro P, Petrone N. Asymptotic thermal and residual stress distributions due to transient thermal loads. *Fatigue and Fracture of Engineering Materials and Structures*. 2009;**32**:936-948
- [14] Ferro P. The influence of phase transformations on the asymptotic residual stress distribution arising near a sharp V-notch tip. *Modelling and Simulation in Materials Science and Engineering*. 2012;**20**:085003

- [15] Meneghetti G, Lazzarin P. The peak stress method for fatigue strength assessment of welded joints with weld toe or weld root failures. *Welding in the World*. 2011;**55**:22-29
- [16] Williams ML. Stress singularities resulting from various boundary conditions in angular corners of plates in tension. *Journal of Applied Mechanics*. 1952;**19**:526-528
- [17] Gross B, Mendelson A. Plane elastostatic analysis of V-notched plates. *International Journal of Fracture Mechanics*. 1972;**8**:267-276
- [18] Seweryn A. Brittle fracture criterion for structures with sharp notches. *Engineering Fracture Mechanics*. 1994;**47**:673-681
- [19] Nui LS, Chehimi C, Pluvinage G. Stress field near a large blunted tip V-notch and application of the concept of the critical notch stress intensity factor (NSIF) to the fracture toughness of very brittle materials. *Engineering Fracture Mechanics*. 1994;**49**:325-335
- [20] Fett T. Failure of brittle materials near stress singularities. *Engineering Fracture Mechanics*. 1996;**53**:511-518
- [21] Dunn ML, Suwito W, Cunningham S, May CW. Fracture initiation at sharp notches under mode I, mode II, and mild mixed mode loading. *International Journal of Fracture*. 1997;**84**:367-381
- [22] Gómez FJ, Elices M. A fracture criterion for sharp V-notched samples. *International Journal of Fracture*. 2003;**123**:163-175
- [23] Planas J, Elices M, Guinea G, Gómez F, Cendón D, Arbilla I. Generalizations and specializations of cohesive crack models. *Engineering Fracture Mechanics*. 2003;**70**:1759-1776
- [24] Kihara S, Yoshii A. A strength evaluation method of a sharply notched structure by a new parameter, The equivalent stress intensity factor. *JSME International Journal Series A Solid Mechanics and Material Engineering*. 1991;**34**:70-75
- [25] Boukharouba T, Tamine T, Niu L, Chehimi C, Pluvinage G. The use of notch stress intensity factor as a fatigue crack initiation parameter. *Engineering Fracture Mechanics*. 1995;**52**:503-512
- [26] Verreman Y, Nie B. Early development of fatigue cracking at manual fillet welds. *Fatigue and Fracture of Engineering Materials and Structures*. 1996;**19**:669-681
- [27] Lazzarin P, Tovo R. A notch intensity factor approach to the stress analysis of welds. *Fatigue and Fracture of Engineering Materials and Structures*. 1998;**21**:1089-1103
- [28] Lazzarin P, Livieri P. Notch stress intensity factors and fatigue strength of aluminium and steel welded joints. *International Journal of Fatigue*. 2001;**23**:225-232
- [29] Atzori B, Meneghetti G. Fatigue strength of fillet welded structural steels: Finite elements, strain gauges and reality. *International Journal of Fatigue*. 2001;**23**:713-721
- [30] Lazzarin P, Lassen T, Livieri P. A notch stress intensity approach applied to fatigue life predictions of welded joints with different local toe geometry. *Fatigue and Fracture of Engineering Materials and Structures*. 2003;**26**:49-58

- [31] Lazzarin P, Sonsino CM, Zambardi R. A notch stress intensity approach to assess the multiaxial fatigue strength of welded tube-to-flange joints subjected to combined loadings. *Fatigue and Fracture of Engineering Materials and Structures*. 2004;**27**:127-140
- [32] Nisitani H, Teranishi T. KI value of a circumferential crack emanating from an ellipsoidal cavity obtained by the crack tip stress method in FEM. In: Guagliano M, Aliabadi MH, editors. *Proceedings of 2nd International Conference on Fracture and Damage Mechanics*; 2001
- [33] Nisitani H, Teranishi T. KI of a circumferential crack emanating from an ellipsoidal cavity obtained by the crack tip stress method in FEM. *Engineering Fracture Mechanics*. 2004;**71**:579-585
- [34] Meneghetti G, Lazzarin P. Significance of the elastic peak stress evaluated by FE analyses at the point of singularity of sharp V-notched components. *Fatigue and Fracture of Engineering Materials and Structures*. 2007;**30**:95-106
- [35] Meneghetti G, Guzzella C. The peak stress method to estimate the mode I notch stress intensity factor in welded joints using three-dimensional finite element models. *Engineering Fracture Mechanics*. 2014;**115**:154-171
- [36] Meneghetti G. The use of peak stresses for fatigue strength assessments of welded lap joints and cover plates with toe and root failures. *Engineering Fracture Mechanics*. 2012;**89**:40-51
- [37] Meneghetti G. The peak stress method for fatigue strength assessment of tube-to-flange welded joints under torsion loading. *Welding in the World*. 2013;**57**:265-275
- [38] Meneghetti G, Campagnolo A, Berto F. Fatigue strength assessment of partial and full-penetration steel and aluminium butt-welded joints according to the peak stress method. *Fatigue and Fracture of Engineering Materials and Structures*. 2015;**38**:1419-1431
- [39] Meneghetti G, Guzzella C, Atzori B. The peak stress method combined with 3D finite element models for fatigue assessment of toe and root cracking in steel welded joints subjected to axial or bending loading. *Fatigue and Fracture of Engineering Materials and Structures*. 2014;**37**:722-739
- [40] Meneghetti G, De Marchi A, Campagnolo A. Assessment of root failures in tube-to-flange steel welded joints under torsional loading according to the peak stress method. *Theoretical and Applied Fracture Mechanics*. 2016;**83**:19-30
- [41] Meneghetti G, Campagnolo A, Rigon D. Multiaxial fatigue strength assessment of welded joints using the peak stress method—Part I: Approach and application to aluminium joints. *International Journal of Fatigue*. 2017;**101**:328-342
- [42] Meneghetti G, Campagnolo A, Rigon D. Multiaxial fatigue strength assessment of welded joints using the peak stress method—Part II: Application to structural steel joints. *International Journal of Fatigue*. 2017;**101**:343-362

- [43] Colussi M, Ferro P, Berto F, Meneghetti G. The peak stress method to calculate residual notch stress intensity factors in welded joints. *Fatigue and Fracture of Engineering Materials and Structures*. DOI: 10.1111/ffe.12757 (Published online)
- [44] Feng Z. *Processes and Mechanisms of Welding Residual Stress and Distortion*. New York: Woodhead Publishing; 2005
- [45] Leblond JB, Devaux J. A new kinetic model for anisothermal metallurgical transformations in steels including effect of austenite grain size. *Acta Metallurgica*. 1984;**32**:137-146
- [46] Koistinen DP, Marburger RE. A general equation prescribing extent of austenite-martensite transformation in pure iron-carbon alloys and carbon steels. *Acta Metallurgica*. 1959;**7**:59-68
- [47] Goldak J, Chakravarti A, Bibby M. A new finite element model for welding heat sources. *Metallurgical Transactions B*. 1984;**15**:299-305

IntechOpen

